Journal of Cleaner Production 149 (2017) 999–1010

Contents lists available at ScienceDirect

Journal of Cleaner Production

journal homepage: www.elsevier.com/locate/jclepro

A combined photovoltaic and novel renewable energy system: An optimized techno-economic analysis for mining industry applications

Eduardo Vyhmeister [a], Cristina Aleixendri Muñoz [b], José Miguel Bermúdez Miquel [b], Javier Pina Moya [b], Carlos Fúnez Guerra [c], Lourdes Rodríguez Mayor [d], Alex Godoy-Faúndez [e], Pablo Higueras [f], Carmen Clemente-Jul [g], Héctor Valdés-González [h], Lorenzo Reyes-Bozo [h, *]

[a] Departamento de Energía y Mecánica, Universidad de las Fuerzas Armadas, ESPE, extensión Latacunga, Ecuador
[b] Departamento de Ingeniería y Desarrollo, Bound4blue S.L., España
[c] Centro Nacional del Hidrógeno, Puertollano, España
[d] Centro de Excelencia de Investigación en Arquitectura, Ingeniería y Diseño, Universidad Europea de Madrid, Madrid, España
[e] Centro de Investigación en Sustentabilidad y Gestión Estratégica de Recursos, Facultad de Ingeniería, Universidad del Desarrollo, Santiago, Chile
[f] Departamento de Ingeniería Geológica y Minera, Universidad de Castilla-La Mancha, Almadén, Ciudad Real, España
[g] Departamento de Energía y Combustibles, Universidad Politécnica de Madrid (UPM), Madrid, España
[h] Universidad Central de Chile, Santiago, Chile

ARTICLE INFO

Article history:
Received 2 October 2016
Received in revised form
18 February 2017
Accepted 18 February 2017
Available online 22 February 2017

Keywords:
Copper mining industry
Renewable energy
Photovoltaic energy
Economic analysis
Optimization system

ABSTRACT

The productivity of the mining industry in Chile, currently the main driver of Chilean economy, is closely tied to foreign demand for ores. Ore-processing is known for involving energy–intensive processes, such as comminution, concentrating and cathodic processes. As mining activities take place in the arid north of Chile, they are affected by water scarcity. Water shortage has forced the industry to pump desalinated seawater up to mining sites over 2000 m above sea level, further increasing electricity consumption. Given these energy needs, and the fact that electrical energy supply in the north of Chile is based on fossil fuels, it is important to consider the use of renewable energies as environment-friendly and economic alternatives. The aim of this work is to evaluate, by an optimized techno-economic analysis, the use of photovoltaic and a novel wind-based technology to supply at least 10% of the current and the predicted electrical energy requirements of the mining industry in the Antofagasta region. A combination of an optimization problem and technical evaluation was performed using Matlab to obtain the optimal number of solar and wind-based technology units in a case study. Total energy generation from a novel wind-based technology unit is 67,616 MWh/y, corresponding to $14.45 \cdot 10^6$ Nm^3 (1298 t) of hydrogen and $7.41 \cdot 10^6$ Nm^3 (10,323 t) of oxygen after electrolytical transformation. Considering a 65% efficiency of the combined cycle fed with hydrogen and oxygen, 28,133 MWh/y of electrical energy would be obtained. For the cases studied the cost of energy from the combined system was estimated to be between 0.255 US$/kWh and 0.273 US$/kWh, slightly higher than the average energy regional cost. According to the analysis, the renewable energy system could be a sustainable alternative to supply economic green energy to the mining industry in Chile.

1. Introduction

Chile is one of the most economically competitive countries in Latin America, a new Organization for Economic, Cooperation, and Development (OECD) member, and considered a high-income country due to high Gross Domestic Product (over US$22,000 per capita; The World Bank, 2016). Agriculture and mining activities, together with services, are the principal drivers of Chilean economic growth (Rehner et al., 2014). The mining industry is mainly located in the north of the country, in the mountainous region of the Atacama Desert, with the Antofagasta region producing almost half of the copper (53% in 2014, as estimated by Cochilco, 2016).

* Corresponding author.
E-mail address: lorenzo.reyes@ucentral.cl (L. Reyes-Bozo).

http://dx.doi.org/10.1016/j.jclepro.2017.02.136
0959-6526/

Nomenclature

dDF	Driving force kg m/s^2
dL	Lift force kg m/s^2
dD	Drag force kg m/s^2
F_H	Turbine drag resistance kg m/s^2
F_v	Viscous resistance kg m/s^2
F_w	Wave resistance kg m/s^2
F_{cr}	Model-ship correlation resistance kg m/s^2
m_{ship}	Ship mass kg
v_{ap}	Apparent wind velocity m/s
v_t	Wind velocity m/s
v_b	Ship velocity m/s
g	Gravity m/s^2
γ	Pointing angle Degree
β	Apparent wind angle Degree
ρ_{air}	Density of air kg/m^3
ρ_{water}	Density of water kg/m^3
Vu	Volume of the Hull underbody m^3
S_{wings}	Surface of the wingsail m^2
S_r	Turbine surface m^2
S_{wet}	Hull wetted surface m^2
D	Ship draft M
Re	Reynolds number –
Fr	Froude number –
$c1$	Hull characteristic parameter of wave resistance –
$c2$	Hull characteristic parameter of wave resistance –
$c5$	Hull characteristic parameter of wave resistance –
$m1$	Hull characteristic parameter of wave resistance –
$m2$	Hull characteristic parameter of wave resistance –
λ	Hull characteristic parameter of wave resistance –
α_C	Temperature power coefficient %
η_A	Availability factor %
η_F	Derate factor %
η_m	Module efficiency %
ε	Average Chilean inflation %
R	Discount rate %
I_k	Incident Irradiation in month k kW h/m^2 d
E_B	Energy generated per ship kW/ship
E_P	Energy generated per m^2 of solar panels kW/m^2
E_{req}	Electrical energy requirement kW
P	Power of hydroturbine kW
T_{cell}	Cell temperature °C
T_{amb}	Ambient temperature °C
C_p	Hydroturbine power coefficient –
C_L	Lift coefficient –
C_D	Drag coefficient –
C_t	Thrust coefficient –
C_v	Viscous resistance coefficient –
C_A	Correlation allowance coefficient –
$CAPEX_{B,i}$	CAPEX per unit of ship to year i US$
$OPEX_{B,i}$	OPEX per unit of ship to year i US$
$CAPEX_{P,i}$	CAPEX per m^2 of solar panel to year i US$
$OPEX_{P,i}$	OPEX per m^2 of solar panel to year i US$
$C_{j,ref}$	Cost Reference for wingsails and hydroturbines US$
C_j	Cost information US$
N_B	Number of ships –
N_P	Number of panels –
n	Wingsail numbers –
n_b	Accumulated number of ships –
C_{learn}	Learning coefficient –

This industrial sector provides around 20% of the gross domestic product and is worth almost 60% of Chilean exportations.

The mining industry is a large energy consumer (around 35% of total electricity) according to the Chilean Statistical Institute and Cochilco statistics on average, energy costs account for nearly 50% of mine operating costs (Cochilco, 2016). Hence, the industry's profitability is highly susceptible to energy prices. The elevated energy requirements are partly due to the continual, energy-intensive, ore processing operational units (especially in the comminution, concentrating, and cathodic processes) and, at the same time, water processing. The need for water in mining processes substantially adds to energy requirements since the industry is mainly located in the extremely arid Atacama Desert, an area that has seen persistent drought over the last ten years. Water Given these conditions, the industry has been forced to obtain water from desalination; energy is required for desalination of seawater and to pump the water up to the pits at a height of 2000 m above sea level. Water and its exploitation is a constant concern in the region, given its limited existence and climate changes (Oyarzún and Oyarzún, 2011; Rivera Salazar, 2012).

To meet energy requirements, the country is dependent on fossil fuels. The electricity is mainly supplied by the North Interconnected System, which in 2015 reached an installed electricity generation capacity of 3968 MWh. This system is based on thermoelectric generation and combined cycles (coal 49%, natural gas 37%, diesel 9% and renewable energy 5%; CNE, 2016).

Fossil fuels in Chile are primarily imported and their use incurs numerous difficulties, such as the logistics of reaching remote areas and increasingly stringent environmental regulations. Also, over the last 15 years, Chile has intensified the use of coal as a source of electricity generation, increasing CO_2 emissions significantly (IEA, 2009). The main energy user (the mining sector), has so far mainly focused on finding ways to improve energy efficiency (Durán et al., 2015; Minenergia, 2013). Nevertheless, the mining industry is currently striving to find alternatives that would respect principles of sustainable development. Renewable energies could be used to replace the present energy sources or to supply the future requirements in the mining industry.

The use of individual sources of renewable energies for constant electric requirements is challenging, given their temporal and irregular nature: solar systems are dependent on sunlight; wind systems cannot operate at high or low wind speeds; biomass are competitive sources of feedstock; biomass production is affected by temperature; and so forth. Nevertheless, by combining different sources (renewable or not), it is possible to supply constant energy to electric networks. Different works (Hiendro et al., 2013; Da Silva et al., 2005; Lau et al., 2010; Himri et al., 2010; Ashok, 2007) have demonstrated the technical and/or economic feasibility of implementing hybrid systems in a variety of contexts. To our knowledge, however, the feasibility of such a system to support the Chilean mining industry has not yet been considered.

Given that the Chilean mining industry is located in the Atacama Desert, the obvious choice for renewable energy is solar power, using photovoltaic technology. Indeed, the regional irradiation indexes range from 5 to 12 kWh/m^2 from winter to summer (Escobar et al., 2014), which are sufficient for the use of photovoltaic technology.

The next seemingly logical choice of renewable energy to

combine with solar power would seem to be wind power, but the relatively low average wind speeds in the area (4 m/s; historical record for Antofagasta Airport and Atacama Desert weather station) and mountainous location of the mines, makes the use of land-based wind energy a difficult task. Prevailing winds in the Pacific Ocean, however, are considerably stronger, reaching average speeds of 10 m/s. This wind energy could be harnessed using a novel non-stationary wind-based technology alternative called "Bound4blue". Since Bound4blue is non-stationary, it does not entail the costs of a distant stationary off-shore station that are related to the transportation or connection of energy; further information about this technology can be found in section 3.

The present work therefore presents an optimized techno-economic analysis of the use of combined photovoltaic and Bound4blue technologies to supply at least the 10% of the current and the predicted electrical energy requirements of the mining industry in the Antofagasta region. The figure of 10% was selected as an option for analysis as it would represent a significant amount, but at the same time would be low enough to enable a smooth transition from thermoelectrical-based supply to a renewable supply. Sharp reductions in energy requirements of fossil fuel supplies could cause damage to different operational units. As mentioned in Bird et al. (2013), in the integration of variable and uncertain renewable energies, it is important to consider the characteristics of the current grid.

To perform the techno-economic analysis, two optimization processes were performed. The first was used to establish the optimum route that the movable wind-based technology should use to optimize the energy harvested. The second optimization used a non-linear analysis to calculate the optimal number of ships and solar panels that should be acquired during the project lifetime (evaluated for 20 years) to supply the mining electrical requirements at a minimum cost (as evaluated by a Net Present Value; NPV). Relative fluctuations of the energy sources, and their monthly variations, were considered in the optimization formulation.

2. Methodology

In the present work the combination of two technologies, photovoltaic and Bound4blue, was considered for the generation of a specific electrical energy requirement. The determination of the units of both technologies was carried out by considering different optimization problems in which the minimum cost and maximum energy harvested were sought in function of temporal, localization, and/or energy requirement restrictions. Specifically, the temporal restrictions involved the inconsistent nature of the natural energy sources (wind speed and irradiation) during the different months of the year and the inexistence of energy to be extracted during the night by the photovoltaic systems. The localization restrictions involved a search for the optimal route that the movable wind-based technology should follow (in function of the available ports in Chile) to maximize the energy harvesting. The energy requirement restrictions involved an even supply of specific quantity of energy during the whole year. For this task, the Matlab (R2010) optimization toolbox was used. The constrained nonlinear minimization was used together with the Interior Point algorithm and the Sequential Quadratic Programming (SQP) algorithm (for comparison) followed by the branch and bound method to solve the Mixed Integer Nonlinear Programming (MINLP) problem.

The cost function is represented as the Net Present Value (NPV) of the project, which considers the capital and operational costs of a constantly increasing demand for energy during the project lifetime (equal to 20 years), as shown in Fig. 1, where the different parts of the proposal methodology are represented.

The energy supplied by each technology was estimated using a technical evaluation which involved force balances, efficiencies, compression, and/or energy conversion, among other evaluations. For the solution of these problems, Matlab (R2010A) was also used.

3. Power generation from Bound4blue technology

Bound4blue technology has been developed by a company of the same name that seeks to develop efficient innovative solutions for maritime transport emission and power consumption; some members of this company are coauthors of the present manuscript. Bound4blue wind-based technology transforms wind energy into the kinetic energy of a movable system, a wind-propelled ship, by using efficient rigid wingsails. The wind-propelled ship possesses hydroturbines which transform the higher-density kinetic energy (produced by the relative velocity of the water and the ship) into mechanical energy. The mechanical energy is transformed into electricity to supply the ship's electricity requirements and to be used by an electrolytic system to produce hydrogen (H_2) and oxygen (O_2) from seawater. The H_2 and O_2 are stored and transported to port where they can be used or sold as a final product. The H_2 can be used as a fuel to produce electrical energy (and heat) in a hydrogen combined cycle, as is the case in the present article.

The power generated by the Bound4blue system is obtained by evaluating four related concepts:

i. The first concept is that the energy harvested in the hydroturbines (fixed to the ship) is obtained by the relative kinetic velocity of the water passing through the turbine rotor.
ii. The second concept is that the ship's relative velocity is obtained by considering a force balance between positive and negative forces; the positive forces are obtained by the wind velocity information and by the considerations of the rigid wing airfoil selection; the negative forces are obtained by considering viscous resistances, wave resistances, the model-ship correlation resistance, and turbines drag resistances.
iii. The third concept is that the energy obtained from the hydroturbine is transformed into electricity which is then used in the electrolysis of sea water. Seawater cannot be used directly in the electrolysis even though its salinity increases

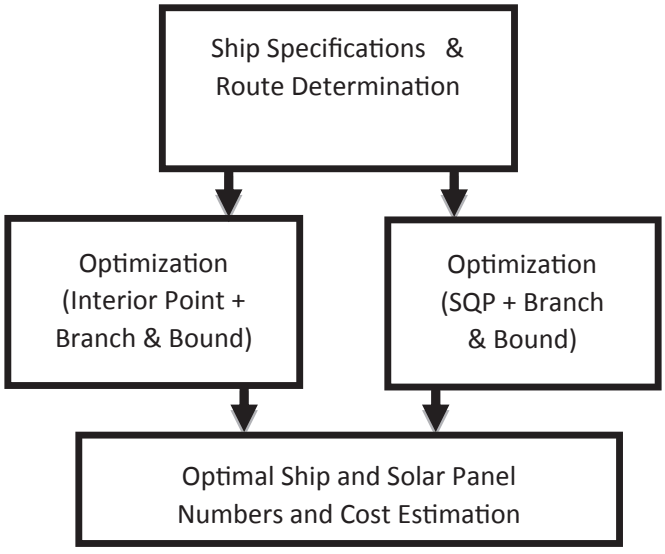

Fig. 1. Main step of proposal methodology.

its electrical conductivity (a positive characteristic of heavily ionized solutions). The different ions present in the water (including chlorine, sodium, sulfate, magnesium, calcium and potassium) can produce different non-desired byproducts in the electrolytic process. The seawater therefore must be treated first, and the electrolyzer must be chosen keeping in mind the limitations of an offshore system. Additionally, the final products (H_2 and O_2) could need further treatment to store them in tanks.

iv. A final concept is that chemical energy produced (H_2 and O_2) must be transformed again into electrical energy in a plant located close the port in order to avoid the installation of expensive pipelines needed for the transportation of H_2 and O_2. This hydrogen combined cycle power plant would supply AC/DC electricity to the network.

Based on the second concept, it is necessary to understand the vector decomposition and the angles involved in the force balance problem. Fig. 2 shows a schematic of the ship considering only one rigid wing sail.

In this figure, v_{ap} is the wind apparent velocity (the vector sum of the real wind velocity and the wind generated by the motion of the ship), β is the apparent wind angle (the angle between the motion, and the apparent wind directions, $\vec{v}_{ap}$); α is the angle of attack (the angle between the airfoil chord line and $\vec{v}_{ap}$); *dL*, *dD*, *dH*, *dR*, and *dDF* are the lift, drag, healing, resulting aerodynamic, and driving (projection of the aerodynamic resulting force to the motion direction) forces, respectively. For a given wind velocity, the factors that determine the terminal sailing speed of the ship, and therefore the power generated by the hydroturbines, are basically the wind forces (previously mentioned) and other resistivity forces, i.e. the thrust of the wing sails and the viscous (F_V), wave (F_W), model-ship correlation (F_{CR}), and the turbine drag (F_H) resistances. Thus, in order to increase the generated power, the wing sails should give as much thrust as possible whereas the resistance should be reduced as much as possible.

The driving force obtained for a selected airfoil depends on β, which is an adjustable parameter that has to be specified in order to obtain the highest power. Theoretically, it is known that the optimum power for a rigid wingsail is obtained when $\beta \approx 45^\circ$ when no interferences exist (based on Fig. 2 and considering the apparent velocity as the hypotenuse of a right angle with real wind and ship wind components as the other components of the triangle). Interferences would be produced when additional wing sails (or other objects, such as tanks) are placed at distances that produce an effect on the wind profile, causing an alteration in the wingsails lift coefficient. By evaluating different β with different number of wingsails, an estimation of $\beta = 60^\circ$ was obtained as the optimum apparent wind angle. To obtain this result, ANSYS 13.0 was used as a simulation tool where the problem was solved as a steady state problem with 15 m/s as wind speed, inviscid as model, air as fluid (density of 1.225 kg/m^3), aluminum as solid, and airfoils as boundary conditions, among other basic specifications. Ignoring the heeling forces (compensated by both the ship hull and the corresponding keel) the equation to apply in the motion direction is Newton's Second Law (Equation (1)).

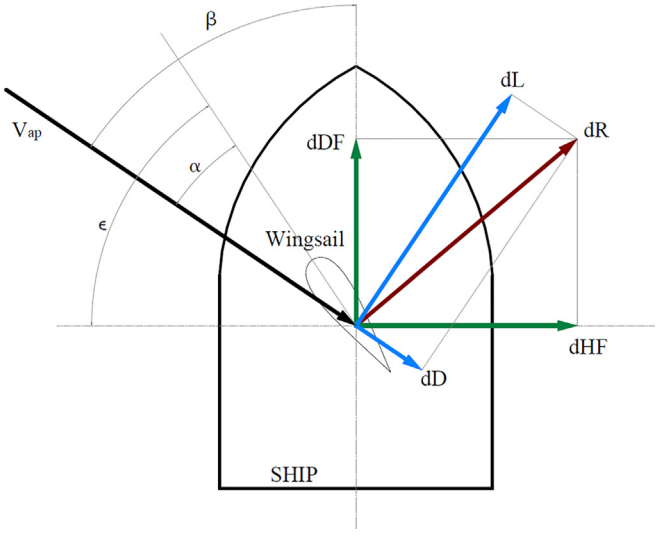

Fig. 2. Forces diagram (adapted from Trillo-Flores, 2012).

$$dDF - F_H - F_v - F_w - F_{cr} = m_{ship} \cdot \frac{dv_b}{dt} \tag{1}$$

As can be seen in Equation (1), the four resistances previously mentioned are considered. Three of them depend on mathematical calculation models (Holtrop and Mennen, 1982) and the fourth corresponds to the turbine drag (Shieves and Crawford, 2010). This method has been chosen because the characteristics of the ship are within the working range of this method and because its reliability is very high compared to other methods.

Considering the previous coordinate system, the apparent wind velocity (v_{ap}) (Equation (2)) and the apparent wind angle (β) (Equation (3)) in a specific time step can be determined (using the cosines theorem) from the ship velocity (v_b), the true wind velocity (v_t) and the pointing angle, formed by the wind vector and the direction of movement (γ). Equation (4) is also derived from the cosines theorem, but in this case the expression is directly dependent on β, which is the correlation used to determinate v_{ap} and v_b from β and v_t information.

$$v_{ap} = \sqrt{v_t^2 + v_b^2 + 2v_t v_b \cos\gamma} \tag{2}$$

$$\beta = arccos\left(\frac{v_t cos\,\gamma + v_b}{v_{ap}}\right) \tag{3}$$

$$v_t = \sqrt{v_{ap}^2 + v_b^2 - 2v_{ap} v_b \cos\beta} \tag{4}$$

The apparent velocity which would be the basis of calculation for the forces involved in the problem can be optimized by setting the most suitable pointing angle. *dDF* is the projection of the aerodynamic forces in the same direction of movement as the vessel. It is calculated using *dL*, and *dD* of the wingsails, as observed in Fig. 2. Equation (5) describes the driving force estimation when the lift and drag forces are evaluated in the same axis of the vessel movement and its corresponding coefficient (C_L and C_D, respectively). As observed in Equation (5), and most of the resistances that are involved in the problem statement (Equations (8), (9), (11) and (14)), a correlation with the kinetic energy ($\sim 1/2v^2$) was used, which is normally made for general aerodynamic considerations.

$$dDF = \frac{1}{2} v_{ap}^2 \cdot S_{wings} \cdot n(C_L \sin\beta - C_D \cos\beta) \tag{5}$$

Equations (6) and (7) show the lift coefficient (C_L) and drag coefficient (C_D). In these equations, ρ_i is the density of the i phase considered (i = water or air) and S_{wings} is the surface of the wingsail.

$$C_L = \frac{dL}{\left(\frac{1}{2}\rho_{air} v_{ap}^2 S_{wings}\right)} \tag{6}$$

$$C_D = \frac{dD}{\left(\frac{1}{2}\rho_{air} v_{ap}^2 S_{wings}\right)} \tag{7}$$

The drag and lift coefficients are functions of the airfoil selection, which in this case corresponds to Eppler 420. As evaluated for this airfoil (with a Reynolds of 10^6), its maximum lift coefficient has a value of nearly 2.3 with drag coefficient of 0.03. The maximum is found at angles of attack of 14°.

The turbine drag, F_H, is described in Equation (8). The drag force slows the ship and thus the total generated power will be smaller. In this equation, S_r is the turbine surface (perpendicular to the flow), and C_t is the thrust coefficient. The C_t considers the forces along the longitudinal axis of the turbine, perpendicular to the rotation plane. The normal coefficient represents the projection of the aerodynamic force into the rotation plane, the one that produces torque to rotate the turbine and from which the power generated is computed. Further drag could be produced depending on the shape of the turbines, as seen for ducted turbines, which could be computed as efficiencies. In the present work, only straight turbines were considered. This implies that the drag coefficient will directly increase the negative forces and positively affect the power generation (i.e. an optimal condition is evaluated).

$$F_H = \frac{1}{2}\cdot\rho_{water}\cdot S_r \cdot v_b^2 \cdot C_t \tag{8}$$

As the ship moves through the water, the fluid friction acts over the hull's wetted surface, causing a drag force called viscous resistance. For low velocities, this resistance represents about 85% of the total resistances; at high speeds, it is about 50%. The semi-empirical equation used to estimate the viscous resistance is expressed in Equation (9), where the viscous resistance coefficient C_v is estimated using a correlation that depends on the fluid dynamic of the system and a form factor k (Equation (10)) that depends on the hull shape ($k = 19(V_u/LWL^2D)^2$), where V_u is the volume of the hull underbody, LWL the ship length, and D is the ship draft.

$$F_v = \frac{1}{2}\cdot\rho_{water}\cdot S_{wet}\cdot v_b^2 \cdot C_v \tag{9}$$

$$C_v = \frac{0.075}{(\log_{10}R_e - 2)^2}\cdot(1+k) \tag{10}$$

In Equation (10), the Reynolds number is estimated using the ship length as the characteristic dimension and the properties of water (water kinematic viscosity equals to 1.08 $m^2\cdot 10^{-6}$/s). The model-ship correlation resistance, F_{cr}, describes the effect of the hull roughness and the still-air resistance. It represents over 10% of the total resistance for a Froude number of 0.3. Its representation is presented in Equation (11), where C_A is the correlation allowance coefficient, the expression of which can be found in Holtrop and Mennen (1982).

$$F_{cr} = \frac{1}{2}\cdot\rho_{water}\cdot v_b^2 \cdot S_{wet}\cdot C_A \tag{11}$$

The waves the ship creates when it moves through the water are produced by the bow and the stern and propagate outwards from the ship. There are two kinds of wave patterns, i.e. the divergent waves and the transverse ones. Wave resistance is affected by beam to length ratio, displacement, shape of the hull, and Froude number. It increases rapidly with the velocity as the transverse wave length approaches the ship's length.

The wave resistance expression is shown in Equation (12). In this equation g is the gravity and $c1$, $c2$, $c5$, $m1$, $m2$ and λ are coefficients that depend on the geometrical characteristics of the hull, as well as in the Froude number (Fr, Equation (13)). The wave resistance is due to the energy transmitted to the water to generate the waves, i.e. energy is lost by the vessel. The contribution of wave resistance to the total resistance is approximately 27% for a Froude number of 0.3. However, as speed is increased, the value of the wave resistance also increases.

$$F_w = c1\cdot c2\cdot c5\cdot V_u\cdot \rho_{water}\cdot g\cdot exp\left(m1\cdot Fr^{d} + m2\cdot\cos\left(\lambda\cdot Fr^{-2}\right)\right) \tag{12}$$

$$F_r = \frac{v_b}{\sqrt{g\cdot LWL}} \tag{13}$$

The coefficient $c2$ will be fixed and have a value of 1, as it depends on the transversal section of the bulbous bow. The calculation of the coefficients is based on Holtrop and Mennen (1982).

The combinations of Equations (1) and (4–13) allows the determination of the ship's velocity in function of the wind speed and β. The differential equation and equations create a system that can easily be solved by different numerical methods or specialized software. The output of the differential algebraic equation system is mainly the instantaneous velocity that can be used to estimate the power extracted from the hydroturbines (as described in Equation (14)). The coefficients involved in each of the previous equations and further information is presented in Table 1.

$$P = \frac{1}{2}\cdot\rho_{water}\cdot S_r\cdot v_b^3\cdot C_p \tag{14}$$

The hydroturbine generated power is transformed into electricity. The efficiency of this conversion is in the order of 95% (Radovic and Schobert, 1991). The resulting electrical energy used is further segmented by considering that 2.5% of the obtained electricity would be used in the ship's electrical components.

It is essential that the electrolyzer selected to transform seawater to H_2 and O_2 can use a process that is technically feasible off-shore. As discussed in the work of Meier (2014), there are four technologies that can be used in water electrolysis: brine electrolysis, alkaline electrolysis, Polymer Electrolyte Membrane (PEM) electrolysis, and Solid Oxide Electolyzer Cell (SOEC). The brine electrolysis is described as a cell for caustic soda production with a smaller molar production rate of hydrogen (Abdel-Aal et al., 2010). Since no oxygen is formed (which is needed later for the production of energy in fuel cell processes) its application was not considered. The alkaline electrolysis uses a potassium hydroxide solution, which would imply a requirement of storage and fungible material, making its application unfeasible. Between the PEM and SOEC electrolyzers, as discussed by Meier (2014), the technologies are alike in that they both need a pure water source and, in their optimal conditions, produce similar H_2 flow rates; however, the SOEC possesses higher efficiencies, uses relatively cheaper materials, requires higher energy and is technically more complex. Since the SOEC has several technological considerations that make its use complex, the PEM electrolyzer was considered for evaluation in the present work; in addition, the PEM electrolyzer can easily be found on the market with considerable conversion efficiencies (in this work a Silyzer 200 of SIEMENS was considered; 4.65 kWh/Nm^3 H_2). Even though the PEM can produce similar results to the SOEC, there is still a gap in energy recovery between the two technologies that

Table 1
Input values selected.

Parameter	Value	Units
Length at flotation line	295.96	m
Beam	50	m
Draught	17	m
Volume of the hull underbody	205,118.3	m^3
Longitudinal position of the center of buoyancy forward of 0.5 L as a percentage of L	3.98	%
Vessel's wet surface	21,255.85	m^2
Midship section coefficient	0.996	–
Waterplane area coefficient	0.882	–
Stern form coefficient	0	–
Immersed transom surface	1.71	m^2
Vessel's weight	210,246,000	kg
Loading capacity	147,862	m^3
Wingsails surface	2550	m^2
Number of wingsails	8	–
Lift coefficient of the wingsail	2.03	–
Drag coefficient of the wingsail	0.05	–
Cross-sectional area of the turbine	78.53	m^2
Turbine thrust coefficient	0.95	–
Turbine power coefficient	0.6	–
Number of turbines	2	–
Water density	1.025	kg/m^3
Air density	1.225	kg/m^3
Gravity acceleration	9.81	m/s^2
Cinematic viscosity	$1.19 \cdot 10^{-6}$	m^2/s

was not considered, which could mean that the SOEC may be a better option in the future.

The remaining energy was considered to be used in the electrolysis and compression of the gaseous products (set to 35 bar, as stated in the electrolyzer specifications). To precisely define how many cubic meters will be obtained, the compression rate had to be considered, since it affects the time needed to fill the tanks.

To calculate the total power, or m^3 of hydrogen and oxygen produced by the vessel, it was necessary to develop a calculation which used NOAA meteorological data to estimate the optimum vessel route. The data was specifically used to predict, with the help of the vessel speed and pointing angle in every possible direction, the maximum distance covered by the ship in a time lapse of 6 h. This means that the program will iterate several times (calculate optimum trajectory - move for 6 h - calculate optimum trajectory) and then generate a route with the maximum traveled distance, which is the same as the maximum power acquired by the turbines and the hydrogen production rate. For the general calculations, specific ports were evaluated as starting and finishing points in the iteration.

Finally, the program selects the fastest route between all the possible ports. Fig. 3 shows the optimal route obtained (which starts and finishes in the Huasco port (−28.4667, −71.25)). Fig. 4 shows an example of the regional wind speeds (obtained from the Vortex Online Wind Modelling Software, VOWM). The wind conditions were evaluated as those reported for the 3rd July, 2016. As stated in VOWM, which is based on wind numerical models from the National Oceanic and Atmospheric Administration (www.noaa.gov) and European Center for Medium-Range Weather Forecasts ECMWF information (www.ecfmwf.int), the medium surface velocity in the studied area was around 11 m/s. It was assumed that the case studied contemplates the variability of the winds throughout the year.

For the simulated route, the load factor (energy generated vs total energy generation capabilities at nominal power for the average wind speed in the route) was 61%, considering the losses at the beginning and at the end of the route. It has been checked that starting from a port situated at southern location, the load factor can be increased to values even higher than 70%.

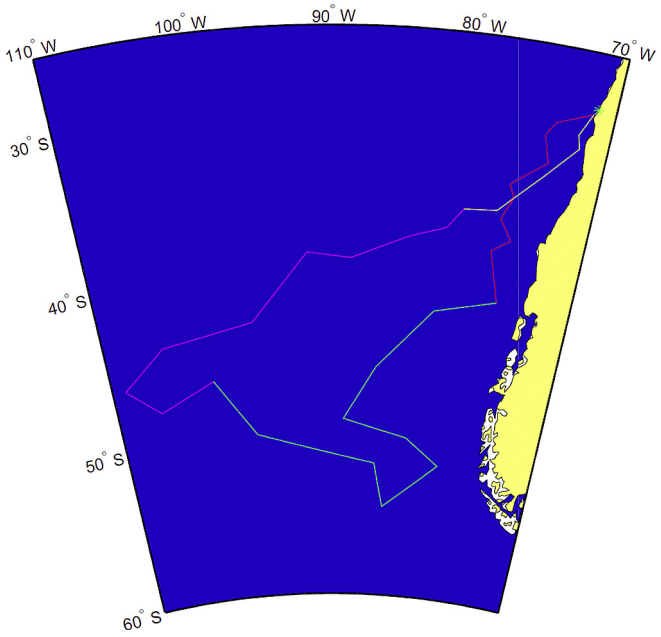

Fig. 3. Optimum route obtained from Huasco port.

As evaluated by the program with the fixed departure date (3rd July, 2016), the duration of the route was 69 days. The total power generated per route was of 13,800 MWh, which corresponds to a generation of $2.96 \cdot 10^6$ Nm^3 (266 t) of hydrogen and $1.48 \cdot 10^6$ Nm^3 (2115 t) of oxygen. So, the selected vessel would lead to the production of 73,000 MWh/y, which corresponds to $15.6 \cdot 10^6$ Nm^3 (1402 t) of hydrogen and $7.8 \cdot 10^6$ Nm^3 (11,146 t) of oxygen. If we consider a loss of 5% from converting mechanical energy to electrical energy and consider a loss of 2.5% for the energy consumption of the ship, the total generation per ship in the year is 67,616 MWh/y, corresponding to $14.45 \cdot 10^6$ Nm^3 (1298 t) of hydrogen and $7.41 \cdot 10^6$ Nm^3 (10,323 t) of oxygen.

The final stage in the evaluation is the conversion of the

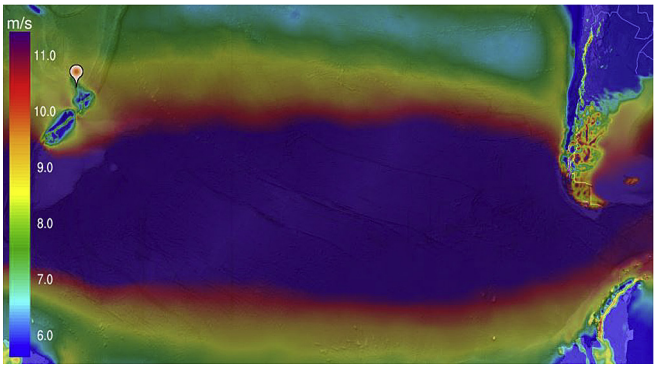

Fig. 4. Vortex online wind modelling medium winds near Chile.

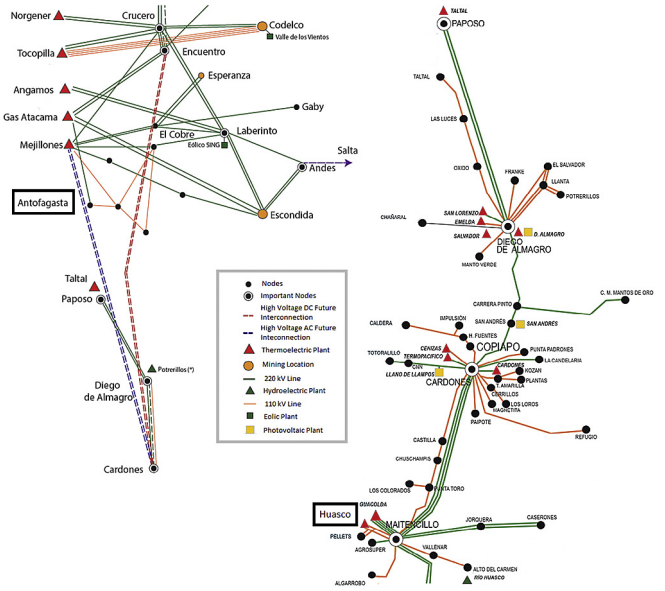

Fig. 5. Chilean electrical grid, projects under development, and principal mining locations.

generated hydrogen and oxygen into useful electricity. For this task, a hydrogen combined cycle with a 60% efficiency was considered (Khartchenko and Kharchenko, 2013; Chiesa et al., 2005). If we consider that the combined cycle is fed with pure oxygen instead of air, the efficiency of the combined cycle will increase by 5%, reaching 65% efficiency.

As discussed above, each ship generates 67,616 MWh/y, which corresponds to 1298 t of hydrogen. Each kilogram of hydrogen contains 33.33 kWh of energy; therefore, 28,133 MWh/y of electrical energy would be obtained. Considering a constant production throughout the year, each ship can provide 3.211 MWh of electrical power.

As stated, the power plant generation was considered to be located in the Huasco port. To transport electricity between the Huasco port and Antofagasta, the existing power grid was considered. The distance between the two points is around 1500 km. Losses due to power transmission to the power level and the distance are around 10% (Weimers, 2014; Vaillancourt, 2014). Hence, the electric power that each ship brings to Antofagasta is of 2.89 MWh per hour. It must be highlighted at this point that the electricity supply in Chile is subdivided in four interconnected networks; the northern grid (Sistema Interconectado del Norte Grande, SING, ~19% of national generation), the central grid (Sistema Interconectado Central, SIC, ~68.5% of national generation and supply of 93% of the Chilean population), and two southern grids (Aysén grid and Magallanes grid). Most of the Chilean population is supplied by the SIC and most of the energy in the north part of the country is fed to the industry. Currently SING and SIC are not connected but, as observed in Fig. 5, there are different projects under development to bring about a connection (that have been advanced up to a 60%, as reported in September of 2016 by the Chilean Ministry of Energy). The SING and SIC will be connected between Mejillones and Cardones by an AC one direction (SING to SIC) interconnection and by a connection between Encuentro and Cardones by a DC bidirectional interconnection (Salinas, 2014). Fig. 5 describes the networks involved and includes the principal locations (as marked in squares) considered in the present work. Furthermore, the principal mining and different plants locations that can incorporate low-energy producing renewable plants have been included.

The efficiency of the system was estimated as 34.68% for the complete cycle - hydrogen and oxygen generation, hydrogen and oxygen storage, and the transformation of hydrogen and oxygen into electricity and the transport of electrical energy. Even though a full comparison of this efficiency level with that of an off-shore wind turbine is beyond the scope of the present article, they can be roughly compared as follows. As a maximum, by using the Betz's law, a 59.3% of the kinetic energy could be harvested from the wind kinetic energy. Typical systems are in the order of 70%–80% of the Betz limits. An off-shore system it would have power losses due to the transmission of electricity from the offshore site and to other sources that are not considered. Given only these considerations (a 75% of Betz limit, and 15% of transmission loss), an efficiency in the order of 37.8% could roughly be estimated, which is not far from the evaluation performed for the Bound4blue system.

4. Power generation from photovoltaic source

The power generated from the photovoltaic system was obtained by considering a specific type of photovoltaic panels (Type: polycrystalline, Brand: KOMES, Model: KM(P)240) in conjunction with the monthly solar irradiation information (Escobar et al., 2014). Of the different technical data for the panels, those used for the calculations are the module efficiency of $\eta_m = 14.7\%$, module size of $1650 \times 990 \times 50$ mm^3, nominal operating cell temperature of 47 ± 2 °C, temperature coefficient of $-0.35\%/°C$, a temperature power coefficient o $\alpha_C = -0.47\%/°C$, and 60 cells per module.

Table 2 shows the monthly information for irradiation and temperature in Antofagasta which is used to estimate temperature derating (efficiency loss due to temperature effects which is expressed by a coefficient called the derate factor; see Equation (15)) and the final monthly average energy generation per square meter of photovoltaic modules. The monthly information describes the average daily energy that is irradiated per square meter close to the Antofagasta city. The temperature used to estimate the temperature derate factor was the average temperature reported plus 20 °C in order to approximate maximum temperatures of the local area. The monthly average energy generated was obtained by using the expression in Equation (15), where the first term in brackets corresponds to the temperature derate factor, η_A is the availability factor (95%) which considers maintenance of the photovoltaic modules, η_F is the derate factor (75%) that stands for ambient effects that could affect the photovoltaic panel efficiency (such as sand over the panel, climate conditions, among others), and I_k is the incident irradiation in the solar panel during the month k. In order for Equation (15) to be true, the photovoltaic panels would have to be considered to be at ambient temperatures. Given that the

Table 2
Monthly solar irradiation and temperature in the Antofagasta city area (adapted from Escobar et al., 2014; Rahn and Garreaud, 2014).

Month	Solar irradiation (kWh/m^2d)	Average temperature (°C)	Monthly average energy generated (kW/m^2)
J	9.0	23.0	0.03595
F	8.5	22.5	0.03404
M	7.5	22.0	0.02991
A	6.2	20.0	0.02495
M	5.0	18.0	0.02049
J	4.6	17.0	0.01894
J	4.7	16.0	0.01945
A	5.5	17.0	0.02265
S	6.5	17.5	0.02670
O	7.9	18.0	0.03237
N	9.1	20.0	0.03691
D	9.4	22.0	0.03910

irradiation could affect this, the temperature derate factor is an approximation that may have a greater impact on photovoltaic solar panel yield according to changes in the irradiation.

$$E_{P,k} = (1 + \alpha_C(T_{cell} - T_{amb}))\eta_A\eta_F\eta_m I_k \quad (15)$$

Similarly to the Bound4blue evaluation, we use the existing power grid for the delivery of the electrical energy. In the previous evaluation, it was necessary to incorporate the approximate distance from the energy plant in Huasco port to Antofagasta. However, in this case, the system will be located in Antofagasta so both evaluated alternatives would suffer a similar efficiency effect. For this reason, and because the relative distances from Antofagasta to the mining locations was shorter, the distance was not considered in the evaluation and would require further analysis.

5. Economic analysis and integrated system optimization

The objective of the economic analysis in the present work is to evaluate the feasibility of using the photovoltaic and Bound4blue technology to provide energy for the Chilean mining industry. At the present, there is a lack of regulations and incentives to use sustainable energy sources in Chile, so the present evaluation would have to be modified if policies and regulations are implemented in the future.

The electricity requirements of the Antofagasta region which are dedicated to the mining industry can be obtained from Cochilco (2016). As reported, constant growth, in the order of 3.8%, can be calculated for the Antofagasta region mining industry electrical consumption (from 2006 to 2015). This electrical consumption (1453.22 MW) was estimated by using the total electrical energy consumption of the mining industry in Chile (84,983 TJ/y for 2015; Cochilco, 2016) and the production percentage of the same region (3108.35 kt/y of fine material produced in the region versus 5764 kt/y produced in Chile).

In the present work, the combination of photovoltaic and the Bound4blue technologies is evaluated to cover 10% of the Antofagasta mining industry electrical requirements. An optimization process was performed to establish the number of ships (N_B) and m^2 of solar panels (N_P) that yearly (from 2016 to 2035) would be required to supply a constantly growing electrical energy from 145.32 MW (for 2016) up to 295.71 MW (2035) at a minimum cost. The cost was estimated based on the Operational Expense (OPEX) and Capital Expense (CAPEX) that would be incurred during the project's life. The NPV was minimized in the optimization problem in order to specify N_B and N_P.

The optimization problem must consider the monthly fluctuations of the natural energy sources. These variations include, for example, the radiation indexes which are higher during the spring-summer season (see Table 2). These variations underline the need for a combination of both technologies to create a robust process.

Based on the previous information, the optimization problem can be stated as described in Equations (16)–(20), where Equation (16) is the objective function to be minimized and Equations (17)–(19) are restrictions (the no-negativity restriction is also included). In these equations, $N_{B,i}$ and $N_{P,i}$ are the number of ships or panels acquired during the year i, respectively; $CAPEX_{B,I}$, $OPEX_{B,I}$, $CAPEX_{P,i}$, and $OPEX_{P,i}$ are the CAPEX and OPEX per unit of ship ($_B$) and m^2 of panels ($_P$) during the year i, respectively; R is the discount rate (considered as a 10%); $\in$ is the average Chilean inflation (4.46%; as from the July 2015–April 2016 Consumer Price Index); E_B and $E_{P,K}$ are the Energy generated per ship and per m^2 of solar panels during the month k (for the ship, a monthly average was estimated from the yearly production estimations); $E_{req,i}$ is the electrical energy requirement of the mining industry during the year i.

Equation (16) describes the total cost during the project lifetime (20 years). As observed in the equation, both costs (CAPEX and OPEX) are modified by the discount rate and the inflation in order to take into account the yearly temporal effects on each of the indexes. The main difference in the CAPEX and OPEX cost considerations is that the latter is multiplied by the total number of ships or m^2 of solar panels accumulated until the year i. Even though Equation (16) seems to have a linear representation, as will be described in the following sections, both the OPEX and CAPEX are non-linear. In the determination of these values, learning curves and scale factors were considered to represent cheaper operational and fixed costs (per unit of ship or m^2 of panels) as the number of units increases.

Equation (17), which is an energetic restriction, establishes that the electrical generation provided by the systems considered (ship or photovoltaic panels) must be superior to the yearly mining industry electrical requirement on each of the k months.

Equations (18) and (19) establish that at least 25% of the energy should come from each of the electrical generation systems considered. This restriction has been added to avoid discontinuities in the electrical supply given by the relative instability of the renewable energetic sources. This information can clearly be confirmed in Table 2, where the photovoltaic peaks can be observed during November to March.

The previous problem corresponds to a MINLP (mixed integer nonlinear programing) since the ships, due to their nature and cost, need to be an integer number. The solar panels, due to their relatively low cost and its implementation, were considered as a continuous variable. In total, the problem statement considers 40 variables ($N_{B,i}$ and $N_{P,i}$), and 500 restrictions.

$$\sum_{i=1}^{20} \frac{(N_{B,i}CAPEX_{B,i} + N_{P,i}CAPEX_{P,i}) \cdot (1 + \varepsilon(i-1))}{(1+R)^{i-1}} + \sum_{i=1}^{20} \frac{\left(\left(\sum_{j=1}^{i} N_{P,j}\right)OPEX_{B,i} + \left(\sum_{j=1}^{i} N_{P,j}\right)OPEX_{P,i}\right) \cdot (1 + \varepsilon(i-1))}{(1+R)^{i-1}} \quad (16)$$

$$S.T.\ for\ i = 1:20 \quad \left(\sum_{j=1}^{i} N_{B,i}\right)E_B + \left(\sum_{j=1}^{i} N_{P,i}\right)E_{P,k} \geq E_{req,,i} \quad \forall\ k = 1:12 \quad (17)$$

$$S.T.\ for\ i = 1:20 \quad \left(\sum_{j=1}^{i} N_{B,i}\right) E_B \geq 0.25 E_{req,i} \tag{18}$$

$$S.T.\ for\ i = 1:20 \quad \left(\sum_{j=1}^{i} N_{P,i}\right) E_{P,k} \geq 0.25 E_{req,i} \quad \forall\ k = 1:12 \tag{19}$$

The ship CAPEX were obtained from the Bound4blue company's information, with eight rigid wingsails (60 m × 20 m) being considered per ship. Additionally, some strategy components of the ships were modified by a learning coefficient (C_{learn} = 0.9; the wingsail systems and the hydroturbines). Table 3 summarizes the costs considered in the present study (as reported by the Bound4blue company) for the first ship manufactured. Although the ship CAPEX are high compared to photovoltaic technology, the relevant point of comparison, as will be presented in the results section, is the cost of the electricity produced.

Equation (20) describes the formulation used to determine the learning effect on the wingsails and hydroturbines components (which would affect the overruns costs and the general expenses). Equation (20) takes into account the accumulated number of ships (up to a maximum of 100; i.e the learning curve was unaffected afterwards), and *ref* stands for the reference cost information (C_j). Finally, an additional 5.63% was included as an overrun, a 6% (over the wingsails) was added as profit, and general expenses equal to 1.6% of the total previous cost were added, as reported by the Bound4blue company.

$$C_j = \frac{\sum n_b^{C_{learn}}}{\sum n_b} C_{j,ref} \tag{20}$$

As explained, the hydrogen generated by the Bound4blue system would be transformed into electricity using a combined cycle plant fueled by hydrogen and oxygen. The CAPEX of a hydrogen combined cycle is 570 US$/kW and the OPEX of a hydrogen combined cycle is 18 US$/kW, according to Khartchenko and Kharchenko (2013) and Chiesa et al. (2005). The hydrogen processed to produce electricity by the hydrogen combined cycle generates 28,133 MWh/y of electrical energy at a plant in or near the port. With these data, the CAPEX and OPEX of the hydrogen combined cycles was estimated to be of US$1,830,270 and US$57,798 per ship, respectively.

The solar panels CAPEX were estimated by considering a Chilean Supplier costs (data obtained from Ningbo Komaes Solar Technology Co.) and regional information. Table 4 specifies the cost per m^2 of panels. It must be considered that the batteries have an average duration of 5 years, so starting from year 6, it was considered that the batteries bought 5 years earlier would be replaced.

Table 3
Ship CAPEX reported by manufacturer (Bound4blue) for 2016.

CAPEX Parameter	COST (US$/ship)
Ship's hull	46,130,116
Wingsail system (×8)	14,882,660
Hydroturbine + transmission	5,849,145
Power generation equipment and regulation system	3,647,389
Electrolysis equipment	7,438,082
H_2 and O_2 Tanks	35,720,575
General overrun	5,983,412
Industrial profit over wingsail system	892,960
General expenses	1,934,746
Total CAPEX (US$/ship)	**122,479,083**

Table 4
Solar Panel CAPEX cost.

Solar Panel Components	Price (US$/m^2)
Polycrystalline Panel	131.26
DC/AC converter cost	16.22
Batteries (US$/m^2) for 1/4 of day	36.98
Land (considering 8 UF/m^2; 1 UF = 25937.85 Chilean Pesos (may-9-2016))	296.43
Movable Structure (for 5 modules)	63.48
Auxiliary costs (10%) (US$/m^2)	24.79
Installation and Construction considering a 20% contingency	54.55

The ship OPEX was estimated by considering time corrections (MS indexes) and scale factors (scale factor equal to 0.6) (Seider et al., 2008) applied to the ship's referenced information (HSH Nordbank, 2010). The OPEX considers manning costs (halved by considering lower salaries in Chile), and insurance costs for hull and machinery, protection, indemnity, loss of hire, and other insurances, maintenance, repair, outfitting costs, lubricants, operating costs, docking and class, management, commission fees (considered equal to 0 for the case study), and other types of costs. The medium cost of the ship OPEX (not considering the hydrogen combined cycle) is around 2.2% of the total investment of the first ship (2,681,369 US$/y). The photovoltaic system OPEX was estimated as a 1% of the total investment (which was regularly updated using an inflation of 4%; VGB PowerTech, 2012).

6. Economic and energy production from the combination of photovoltaic and Bound4blue technology

The previously optimization problem was solved by using Matlab to obtain the optimal N_B and N_P to supply the 10% of the electrical requirement of the mining industry in the Antofagasta region. Table 5 shows the results obtained ($CAPEX_{B,i}$, $CAPEX_{P,i}$, $OPEX_{B,i}$, $OPEX_{P,i}$, and average annual MW produced by the combined system) under two different circumstances (to evaluate the sensibility of the formulated problem). The first number on each grid specifies the results obtained based on the CAPEXs and OPEXs the previously mentioned problem (here and after referred to as the original problem), while the second number specifies the optimization results when the $CAPEX_{B,i}$ was reduced by 20% (here and after referred to as the modified problem). As could be deduced from the previous definitions, the sensibility of the system was evaluated as a function of the ship cost, which would inevitably lead to using one or other of the energy sources under consideration.

As observed in the original problem, 13 ships and almost 5.69 km^2 of solar panels would be required for the first year of the project. During the following years, an increasing number of solar panels and ships would be required to meet the predicted increase in electricity requirements, with almost one ship per year over the whole duration of the project, and from an additional 0.139 km^2 of solar panels in 2017 up to 0.418 km^2 of solar panels in 2035. The irregularity of the numbers obtained (years with 0 ships and small variations in the increasing number of solar panels) is given by solving the problem as a MINLP and the implication that one ship could modify considerably the costs and total energy produced for the stated problem.

It should be highlighted that the results with a 20% CAPEX reduction was obtained with the Interior point algorithm. Similar results were obtained with the SQP algorithm but with a 31% reduction in the $CAPEX_{B,i}$. Regardless of these results, by evaluating the final NPVs it was observed that the Interior Point algorithm

Table 5
Optimal number of ships and solar panels without (first number) and with (second number) sensitive analysis (20% reduction of ship CAPEX). The economic results include the inflation but not the discount rate.

Year	Ships [Units]	Solar Panels [km^2]	$CAPEX_B$ (MUS$)	$CAPEX_P$ (MUS$)	$OPEX_B$ (MUS$)	$OPEX_P$ (MUS$)	Average Electricity (MW)
1	13	5.690	1556.00	3548.80	35.61	35.49	198.82
	37	2.029	3493.20	1265.50	101.34	12.65	164.40
2	1	0.139	124.34	90.17	39.88	37.81	205.64
	1	0.139	98.12	90.17	108.25	14.63	171.23
3	0	0.303	0	203.86	41.42	41.30	214.22
	2	0.000	203.67	0	118.332	15.77	177.01
4	1	0.162	133.78	112.90	46.02	43.96	221.69
	2	0.021	211.08	14.68	128.85	17.13	182.97
5	0	0.326	0	235.92	47.66	47.89	230.93
	1	0.174	109.27	125.57	136.63	19.83	190.77
6	1	0.186	143.21	391.68	52.59	50.93	239.09
	1	0.033	113.01	115.05	144.63	21.52	197.50
7	0	0.351	0	278.09	54.35	55.35	249.05
	2	0.046	233.42	42.14	156.24	23.42	204.59
8	1	0.212	152.62	183.69	59.60	58.83	257.95
	1	0.212	120.44	169.37	164.78	27.13	213.49
9	0	0.379	0	319.56	61.46	63.78	268.68
	2	0.073	248.27	601.54	177.17	29.65	221.36
10	1	0.240	162.03	220.32	67.06	67.76	278.38
	2	0.088	255.67	83.25	189.99	32.48	229.62
11	1	0.255	166.67	527.17	72.86	71.98	288.51
	2	0.103	263.06	196.54	203.25	35.68	238.31
12	0	0.423	0	406.33	74.94	77.84	300.51
	2	0.118	207.44	116.09	216.94	39.27	247.44
13	1	0.287	176.07	293.02	81.08	82.65	311.52
	2	0.134	277.83	135.65	231.08	43.32	257.03
14	1	0.304	180.71	318.23	87.43	87.76	323.02
	3	0.000	427.73	5.31	249.81	45.69	265.69
15	1	0.321	185.35	344.98	94.01	93.20	335.01
	2	0.167	292.54	177.57	264.93	50.67	276.21
16	1	0.339	189.98	701.00	100.80	98.96	347.50
	2	0.186	299.92	314.11	280.49	56.28	287.27
17	0	0.510	0	577.30	103.32	106.65	361.96
	3	0.053	460.86	73.14	300.98	60.01	297.43
18	1	0.377	199.36	444.85	110.44	113.21	375.53
	3	0.072	471.84	96.93	322.13	64.24	308.13
19	1	0.397	204.00	479.64	117.78	120.16	389.67
	2	0.245	321.94	262.37	339.22	71.85	320.85
20	1	0.418	208.63	516.63	125.34	127.54	404.41
	3	0.113	493.89	151.86	361.57	77.41	332.71

produced better results; the NPVs in the limiting conditions (maximum number of solar panels or maximum number of ships) should be similar and, as observed, the SQP underestimated the limiting condition, with a NPV considerably lower than the original problem. This result supports that notion that a 20% reduction in CAPEX would be more than enough to make a transition from one energy source to another (a further explanation is given below).

For the modified problem, about 37 ships and 2.09 km^2 of solar panels would be required for the first year of the project. The following years the numbers will irregularly increase (given by the MINLP formulation) from an additional ship in 2017 up to 3 ships in 2035, and from an additional 0.139 km^2 of solar panels up to 0.113 km^2 of solar panels. The results clearly establish that for the original problem, the solar panels would be the preferred energy source since the panel surface area is the maximum number that can be used to fulfill the system restrictions (i.e. minimum number of ships that can be used). On the other hand, by modifying the ship CAPEX by 20%, the Bound4blue system is established as the preferred energy source, since the number of ships is established as close to its maximum and the solar panel surface area to its minimum. Given the sensitivity of the problem to the ship CAPEX, slight variations in the power outputs, costs, or technologies could lead to prefer one source of energy over the other. The NPVs for the original and modified systems are very close - 9468.3 MUS$ and 9321.9 MUS$ (with the interior point algorithm), respectively (8575.2 MUS$ with the SQP algorithm, which establishes that SQP wrongly predicts the transition from one energy source to another). For the original problem NPV, 88.8% comes from the CAPEX. Similarly, for the modified problem (as solved with the interior point algorithm) 80.5% comes from the CAPEX. This result implies that the ship OPEX is relatively higher.

Additionally, Table 5 shows the average energy produced by both problems under consideration. As observed in the original problem, the average energy produced is higher than the modified problem. This is due to the variable energy output of the solar panels due to temporal fluctuations. For the solar panels case, the minimum happens when the irradiation energy is at its minimum (June) but, for the rest of the year, there will be an over production of energy. As the surface area of the solar panels is increased, the average annual production would considerably increase over the mining industry requirements. On the other hand, in the optional problem, the ship is the preferred energy source and the average energy produced is relatively closer to the requirements.

As observed in Table 5, for the fifth year of the project (year 6 in the table), an increase in the CAPEX of the solar panels can be observed for both problems. This is due to the consideration of the battery lifetime, which is about 5 years, and implies a considerable increase in the CAPEX for the solar panels. In fact, this number will increase every five years (years 11, 16, and so on). This growing CAPEX will inevitably incur a considerable cost to the solar panel

analysis and could lead, depending on the year of the economic evaluation, to the selection of ships a more favorable alternative.

By analyzing the energy generated, it can be observed that the ships produce almost 0.231/1.876 times the energy produced by the solar panels (original/modified problems, respectively); for the first year of evaluation the ships produce, on average, 37.55 MW/106.89 MW (original/modified problems, respectively). The ship OPEX implies an average cost of electricity of 0.108 US$/kWh (independently of the original/modified problems) which is considerably lower than the average regional cost (which is in the order of 0.2 US$/kWh; as observed in market prices). By considering the CAPEX of the first year (and its energy produced) divided over the evaluation period (20 years) and the OPEX costs, the total cost of energy is 0.255 US$/kWh/0.273 US$/kWh (original/modified problems, respectively). The previous results establish that as the number of ships increases, the cost of the electricity production will be slightly increased. Nevertheless, as further ships are incorporated, the cost should be reduced considerably, according to the ship learning curve (consideration made in the ship costs).

Regardless of these results, there are several considerations that could increase or reduce the costs involved in the ship evaluation. The prices could be reduced further since the investment and operational costs of Western Europe, on which the calculations were based, are considerably higher than in South America. In fact, this factor could reduce some of the costs involved by up to a 20%, as observed in the investment site factors (Seider et al., 2008). Furthermore, the depreciation was not included in the analysis, which could affect the NPV of the projects. Additionally, the ship has mainly been considered as being used for energy generation, but it could be used for additional purposes such as transportation, that would generate profit or reduce other expenditures involved in the transport of mining supplies and products. Finally, the evaluation has been made by considering several transformations in the energy production (kinetic-to-mechanical-to-electrical-to-chemical-to-electrical energy conversions); as stated in previous work (Reyes-Bozo et al., 2015), the Bound4blue technology could also be considered a cheaper alternative for hydrogen production (about 30%), so it could partially be self-sustained. These factors clearly establish the advantages of Bound4blue as a sustainable alternative to supply energy to the mining industry in Chile. If governmental incentives or restrictions are implemented in the country, this could lead to an improved acceptance for introduction of technologies such as Bound4blue.

7. Social and environmental benefits

Energy plants fired by fossil fuels are well known for emitting particulate matter that can be dangerous to health, including, for example sulfur dioxide, NO_X, Hg, and particulate matter 2.5. Evidence of this can be found even up to thousands of kilometers downwind of plants (Cohen et al., 2005; Wang et al., 2016). Continual exposure to these pollutants has been linked to elevated health risks for illnesses of the respiratory (asthma, lung disease and cancer), cardiovascular (arterial occlusion, infarct formation) and nervous systems (Cohen et al., 2005) and increased associated morbidity (Pope, 2000). In Chile, there are significant correlations between emissions from the mining, metal processing, paper production and energy industries and increases in health risks in local communities around facilities for cardiovascular and respiratory diseases (Ruiz-Rudolph et al., 2016). Replacing 10% of the current and predicted electrical energy requirements for the mining industry in the Antofagasta region by using the hybrid technology evaluated in this study could bring social, environmental and economic benefits that would contribute to the overall sustainability of the copper mining industry.

8. Conclusions

The use of renewable energies to supply 10% of the current and future electrical requirements of the copper mining industry in the Antofagasta Region of Chile has been evaluated. A hybrid system that comprises two different sources of renewable energy is proposed. The first source is a photovoltaic system that uses solar irradiation in the northern region of Chile. The second is a novel renewable energy system called Bound4blue which harvest wind kinetic energy, using ships with rigid wingsails, to produce as final output electrical energy (by different transformations). In order to perform the economic feasibility study, an optimization problem was stated (min-max problem; minimal cost with maximum energy production). The maximum energy produced was found by obtaining an optimum route to harvest the kinetic energy while the minimum cost evaluated operational and capital costs involved in a global project evaluation over a period of 20 years. The optimal number of ships and solar panels for the first year in a combined system was estimated as 13 ships and 5.75 km^2 of solar panels. If a 20% reduction of the ship capital costs (e.g., costs of wingsails systems and, H_2 and O_2 storage tanks, electrolysis equipment) is made, the combined systems was estimated as 38 ships and 1.92 km^2 of solar panels. The results establish that fluctuations in technology, energy efficiency, and costs could lead to a preferred source of renewable energy for the problem stated. For both scenarios, the energy costs were estimated to be between 0.255 US$/kWh and 0.273 US$/kWh, which are slightly higher than the average regional energy cost.

Evidently this paper presents a simulation of the costs involved in the proposed photovoltaic-Bound4blue hybrid system, and it would be important in the future to carry out a trial run to identify possible shortcomings and practical difficulties. Nonetheless, we consider that the evaluations made in this paper have been extremely thorough, and are therefore confident that this renewable system could partially supply the energy mining requirements in Chile and, at the same time, improve the overall environmental sustainability of the copper mining industry. Given that the costs of such a system are slightly higher than the current regional energy costs, economic support would be crucial for its implementation. Increasing costs of fossil fuels and the growing need for energy independency may lead to the financing of such alternative energy sources in Chile in the near future.

Acknowledgments

The grant to Reyes-Bozo, L. obtained from Universidad de Castilla-La Mancha (“Ayudas para estancias de investigadores invitados en la UCLM para el año 2016”) was greatly appreciated. Additional support came from Universidad Central de Chile (C. Fúnez Guerra).

References

Abdel-Aal, H.K., Zohdy, K.M., Abdel, K.M., 2010. Hydrogen production using sea water electrolysis. Open Fuel Cells J. 3, 1–7.
Ashok, S., 2007. Optimised model for community-based hybrid energy system. Renew. Energ 32 (7), 1155–1164.
Bird, L., Milligan, M., Lew, D., 2013. Integrating Variable Renewable Energy: Challenges and Solutions. National Renewable Energy Laboratory. www.nrel.gov/publications (Accessed 23 November 2016).
Chiesa, P., Lozza, G., Mazzocchi, L., 2005. Using hydrogen as gas turbine fuel. J. Eng. Gas. Turb. Power 127, 73–80.
CNE, Comisión Nacional de Energía, 2016. 2015 energy Statistical Yearbook Chile. Santiago, Chile, p. 126.
Cochilco, Chilean Copper Commission, 2016. Yearbook: Copper and Other Mineral Statistics 1996-2015, Santiago, Chile, p. 170.
Cohen, A.J., Anderson, H.R., Ostro, B., Pandey, K.D., Krzyzanowski, M., Kunzli, N., Gutschmidt, K., Pope, A., Romieu, I., Samet, J.M., Smith, K., 2005. The global

burden of disease due to outdoor air pollution. J. Toxicol. Environ. Health A 68 (13–14), 1301–1307.
Da Silva, E.P., Marín-Neto, A.J., Ferreira, P.F.P., Camargo, J.C., Apolinário, F.R., Pinto, C.S., 2005. Analysis of hydrogen production from combined photovoltaics wind energy and secondary hydroelectricity supply in Brazil. Sol. Energy 78, 670–677.
Durán, E., Aravena, C., Aguilar, R., 2015. Analysis and decomposition of energy consumption in the Chilean industry. Energy Policy 86, 552–561.
Escobar, R.A., Cortés, C., Pino, A., Bueno Pereira, E., Ramos Martins, F., Cardemil, J.M., 2014. Solar energy resource assessment in Chile: satellite estimation and ground station measurements. Renew. Energ 71, 324–332.
Hiendro, A., Kurnianto, R., Rajagukguk, M., Simanjuntak, Y.M., Junaidi, 2013. Tecno-economic analysis of photovoltaic/wind hybrid system for onshore/remote area in Indonesia. Energy 59, 652–657.
Himri, Y., Stambouli, A.B., Draoui, B., Himri, S., 2010. Techno-economical study of hybrid power system for a remote village in Algeria. Energy 33 (7), 1128–1136.
Holtrop, J., Mennen, G.G.J., 1982. An approximate power prediction method. Int. Shipbuild. Prog. 29 (335), 166–170.
HSH Nordbank, 2010. Operating Costs: a Study on the Operating Costs of German Container Ships. Hamburg, Germany.
IEA, International Energy Agency, 2009. Chile: Energy Policy Review 2009, Paris, France, p. 270.
Khartchenko, N.K., Kharchenko, V.M., 2013. Advanced Energy Systems, second ed. CRC Press, Taylor & Francis Group, Boca Ratón, FL, USA.
Lau, K.Y., Yousof, M.F.M., Arshad, S.N.M., Anwari, M., Yatim, A.H.M., 2010. Performance Analysis of hybrid photovoltaic/diesel energy system under Malaysian conditions. Energy 35 (8), 3245–3255.
Meier, K., 2014. Hydrogen production with sea water electrolysis using Norwegian offshore wind energy potentials. Int. J. Energy. Environ. Eng. 5 (104), 1–12.
Minenergia, Ministerio de Energía, 2013. Plan de acción de eficiencia energética 2020 (Action Plan of Energy Efficiency 2020), Santiago, Chile, p. 44.
Oyarzún, J., Oyarzún, R., 2011. Sustainable development threats, inter-sector conflicts and environmental policy requirements in the arid, mining rich, northern Chile territory. Sustain. Dev. 19 (4), 263–274.
Pope, C.A., 2000. Epidemiology of fine particulate air pollution and human health: biologic mechanisms and who's at risk? Environ. Health Perspect. 108 (4), 713–723.
Radovic, L.R., Schobert, H.H., 1991. Energy and Fuels in Modern Society, first ed. McGraw-Hill, New York.
Rahn, D.A., Garreaud, R.D., 2014. A synoptic climatology of the near-surface wind along the west coast of South America. Int. J. Climatol. 34, 780–792.
Rehner, J., Baeza, S.A., Barton, J.R., 2014. Chile's resource-based export boom and its outcomes: regional specialization, export stability and economic growth. Geoforum 56, 35–45.
Reyes-Bozo, L., Aleixendri Muñoz, C., Bermúdez Miquel, J.M., Fúnez Guerra, C., 2015. Bound4blue concept applied to the Chilean mining industry. In: Proceedings of 11th International Mineral Processing Conference (Procemin), Santiago, Chile.
Rivera Salazar, D., 2012. Chile: Environmental, Political, and Social Issues. Nova Science Publisher's, New York, USA.
Ruiz-Rudolph, P., Arias, N., Pardo, S., Meyer, M., Mesías, S., Galleguillos, C., Schiattino, I., Gutiérrez, L., 2016. Impact of large industrial emission sources on mortality and morbidity in Chile: a small-areas study. Environ. Int. 92–93, 130–138.
Salinas, F., 2014. Desventajas de una interconexión SIC-SING en Corriente Alterna, Central Energía. www.centralenergia.cl (Accessed 12 November 2016).
Seider, W.D., Seader, J.D., Lewin, D.R., Widagdo, S., 2008. Product and Process Design Principles: Synthesis, Analysis and Design, third ed. Wiley, USA.
Shieves, M., Crawford, C., 2010. Overall efficiency of ducted tidal current turbines. In: Proceedings of Oceans 2010 MTS/IEEE, Seattle, USA.
The World Bank, 2016. World Bank, International Comparison Program Database. GDP per capita, PPP (current international $). data.worldbank.org/indicator (Accessed 30 July 2016).
Trillo-Flores, N., 2012. Preliminary Study of a Power Generation System Based on Rigid Wing Sails. Universitat Politécnica de Catalunya.
Vaillancourt, K., 2014. Electricity Transmission and Distribution. iea-etsap.org (Accessed 30 July 2016).
VGB PowerTech, 2012. Investment and Operation Cost Figures – Generation Portfolio. VGB PowerTech, Essen, Germany, p. 8.
Wang, F.F., Geng, C.M., Hao, W.D., Zhao, Y.D., Li, Q., Wang, H.M., Qian, Y., 2016. The cellular toxicity of PM2.5 emitted from coal combustion in human umbilical vein endothelial cells. Biomed. Environ. Sci. 29 (2), 107–116.
Weimers, L., 2014. Bulk Power Transmission at Extra High Voltages, a Comparison between Transmission Lines for HVDC at Voltages above 600 kV DC and 800 kV AC. ABB Power Technologies AB, Ludvika, Sweden, p. 9.